Int J CARS (2016) 11:217–229
DOI 10.1007/s11548-015-1248-4

ORIGINAL ARTICLE

Three-dimensional modeling of an individualized functional masticatory system and bite force analysis with an orthodontic bite plate

Fanfan Dai[1] · Longfang Wang[2] · Gui Chen[1] · Si Chen[1] · Tianmin Xu[1]

Received: 10 December 2014 / Accepted: 10 June 2015 / Published online: 25 June 2015

Abstract
Purpose Orthodontic tooth movement is affected by bite forces generated from the masticatory system. This study aims to study three-dimensional (3D) modeling of the individualized functional masticatory system and explore its application in orthodontics.
Methods An individualized masticatory system model containing the craniomaxilla, mandible, 4 pairs of primary masticatory muscles and complete dentition, including roots and precise dental crowns, was developed using 3D images from spiral computed tomography and digital casts. By registering global coordinates and using data transformation, individual movement data for mandibular opening, lateral excursion and protrusion were recorded with an Arcus Digma system and applied to this model to simulate the functional movements of the mandible. Using the finite element method, deformations and displacement of the masticatory muscles were simulated along with the mandibular movements. Under individualized muscle loading, the bite forces of the lower incisors with the orthodontic bite plate were analyzed.
Results Individualized mandibular movements were simulated, and the performance of the masticatory muscles along with the mandibular movements was measured. The bite force generated on the lower incisors with different thicknesses and the orientations of the orthodontic bite plate were acquired.
Conclusion An individualized 3D masticatory system model was constructed using advanced 3D data processing software that integrated 3D images from different sources. Individualized mandibular movement and masticatory muscle performance were simulated using this model. The analysis of the bite force generated on the lower incisors with the orthodontic bite plate suggested that a thickness of 3 mm may be appropriate for clinical use.

Keywords Masticatory system · Mandibular movement · Finite element · Three-dimensional model · Bite force

Introduction

Orthodontic tooth movement is caused not only by the mechanical forces imposed by orthodontists using archwire-bracket systems but also by complex physiological forces generated by the patient's stomatognathic system. The bite force generated by masticatory muscle activity is an important part of this system. Bite force is believed to affect tooth movement and stability, and the anterior component of the bite force is a significant contributor to the mesial drift of teeth and the development of crowded dentition [1,2]; by contrast, bite force may be used by orthodontists for treatment, such as using the flat bite plate to intrude the lower anterior teeth and open the bite [3].

Bite force is thought to be closely related to the craniofacial morphology [4], masticatory muscles [5] and dentition [6], which constitute an individual's masticatory system. Functional disturbances of the masticatory system also affect bite force [7]. Currently, the magnitude and distribution of an individual's bite force can be simply and accurately measured using T-Scan III [8] and Dental Prescale Occluzer systems [9]. However, the direction of the force is not directly measur-

✉ Si Chen
elisa02chen@gmail.com

✉ Tianmin Xu
tmxuortho@163.com

1 Department of Orthodontics, Peking University School and Hospital of Stomatology, Beijing 100081, China

2 Beihang University School of Astronautics, Beijing 100081, China

able during the combined functional activities of the entire masticatory system.

In recent years, multiple studies have used the three-dimensional (3D) finite element (FE) method to simulate the masticatory system [10,11]. With this method, both the magnitude and direction of the bite force can be resolved by applying masticatory muscle forces to the teeth. In addition to a simulation of the masticatory system's functional activity [10], a 3D image-based reconstruction is commonly recommended [11] because the accuracy of a 3D FE model is determined using a geometric model. Otake [12] and Terajima [13] combined a 3D craniomandibular model with mandibular movement data to achieve dynamic simulations of individual mandibular movements. However, they did not explore the relationship between mandibular movement and masticatory muscle function.

In this study, an individualized functional masticatory system model with improved integrity and accuracy was developed by combining data from spiral computed tomography (CT), digital casts and individual mandibular movement records. Mandibular movement and masticatory muscle performance were simulated with the FE method, and the bite forces of the lower incisors with the orthodontic bite plate were analyzed under the individualized masticatory muscle force load.

Materials and methods

Subject

A 23-year-old female volunteer was enrolled under the following inclusion criteria: intact dentition (except the third molar), individual normal occlusion, optimal periodontal health, no obvious facial asymmetry, no temporomandibular disorder, and no history of orthodontic or severe endodontic treatment.

Data collection

3D digital dentition

Upper and lower dental casts with high precision were obtained using polysiloxane impression material (Affinis, Coltène Whaledent Inc., Altstätten, Switzerland) and die stone model material (Type IV high-strength artificial stone, Heraeus Kulzer Inc., South Bend, IN, USA). The occlusal relationship was recorded with maximum clenching in the intercuspal position using the same polysiloxane impression material. The upper and lower casts (occluded and separated), the bite fork, the upper cast with the bite fork in position, and the occlusal relationship record were scanned with a Roland LPX-1200 laser scanner (Roland DG., Hamamatsu, Japan, accuracy ±0.02 mm). All of the scan results were saved as STL files.

3D craniofacial images of bone, muscle and teeth

Craniofacial images were obtained with a 64-slice spiral CT device (PHILIPS Inc., MA, USA) at 150 kV and 230 mA, producing DICOM formatted images. The thickness of each tomographic scan was 1.0 mm. During scanning, the volunteer was instructed to gently bite in the maximum intercuspal position. The DICOM data were imported into a 3D software platform, Amira5.2.2 (Visage Imaging Inc., CA, USA). Using a combination of thresholding and manual segmentation methods (Fig. 1), the craniomaxilla, mandible, 28 teeth (central incisor to second molar in four quadrants) and 4 pairs of masticatory muscles (bilateral temporalis, masseter,

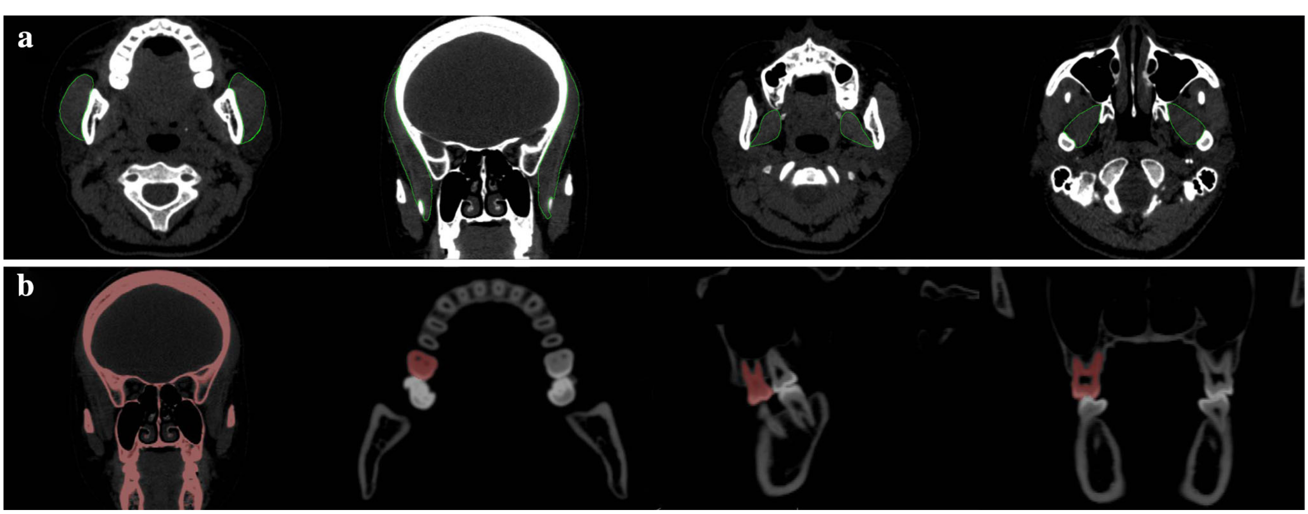

Fig. 1 Segmentation of the muscles (**a**), bone and teeth (**b**) using a combination of thresholding and manual methods

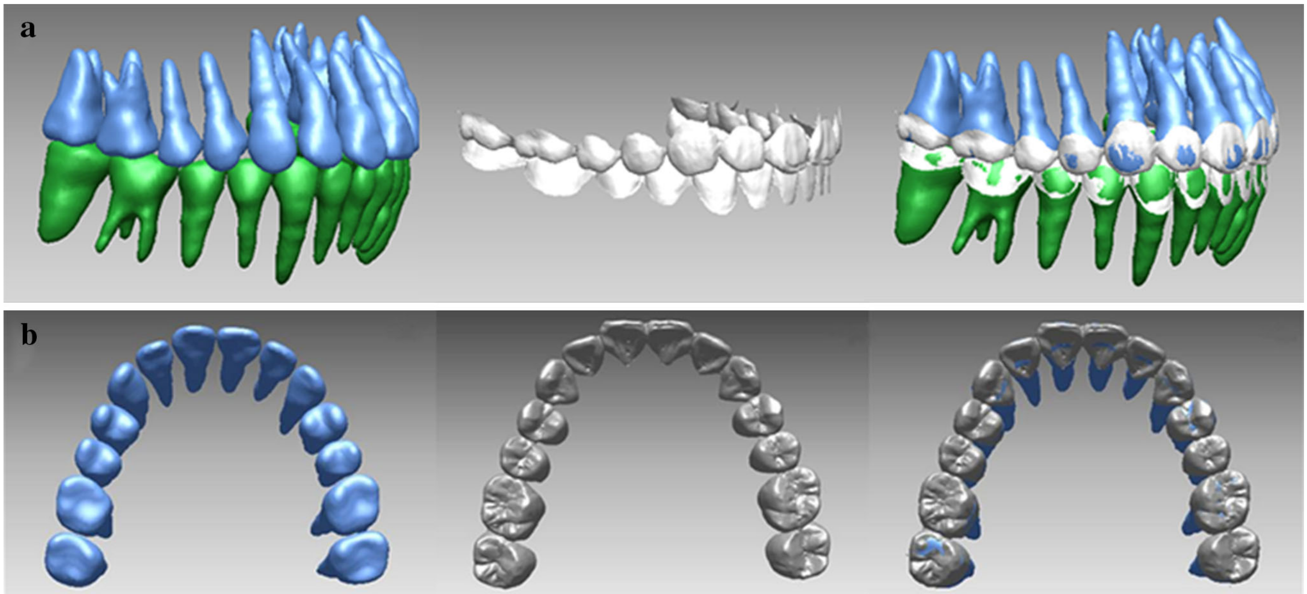

Fig. 2 Registration of the teeth from CT data with the dental crowns from digital casts. **a** Buccal view. **b** Occlusal view

medial pterygoid and lateral pterygoid) were segmented, reconstructed and saved as STL files. The segmentation threshold were 260–3000 HU for bone, 1160–3000 HU for teeth and 30–120 HU for muscles.

3D mandibular movement data

The volunteer's mandibular movements, specifically their maximal interincisal opening, protrusion and lateral excursion, were recorded with a 3D ultrasonic axiograph Arcus Digma system (KaVo, Biberach, Germany, accuracy ±0.1 mm). The Arcus Digma system measured the run times of ultrasonic pulses from three transmitters carried by the mandibular frame to three receivers embedded in a head frame. These times were converted into sequential 3D coordinate value changes for 3 reference landmarks. The data were saved as a TXT file.

Generation of the static masticatory system model

All of the STL files, including the 3D images of the craniomaxilla, mandible, muscles and teeth from the CT and digital casts, were imported into the reverse engineering software Rapidform 2006 (Inus Technology Inc., Seoul, Korea). The 28 independent tooth images, segmented from the CT data, included both crowns and roots, although the crowns were not accurate enough to determine occlusion. Therefore, the CT tooth data and the digital crown data were integrated to solve the problem. First, using a regional registration method, the upper and lower casts were separately registered onto the casts made in occlusion—occlusion was not scanned in detail but was established as the reference frame for the occlusal relationship. Then, the digital crowns with precise occlusal surfaces were segmented and registered onto the teeth reconstructed from the CT data (Fig. 2). The radial basis function (RBF) transformation method [14] was then applied to adjust the CT data toward the digital crowns to compensate for minor image shrinkage from the CT reconstruction. Finally, a static model of the individualized masticatory system was established, including the craniomaxilla, the mandible, 4 pairs of primary masticatory muscles and 28 complete teeth (Fig. 3a, b).

Validation of the static masticatory system model included two parts, the error of occlusion between upper and lower teeth and the error of RBF transformation. The former was performed by comparing the inter-point distance between the upper and lower teeth in the digital casts (DC group) with that of the digital occlusal relationship record (DR group) (Fig. 4). The chosen points were mainly recognizable fossa points that located on the occlusal surface of posterior teeth. Ten pairs of inter-point distances were measured three times by one examiner; the intra-class correlation coefficient for the three repeated measurements was above 0.90 for both groups, and the mean measurements were calculated and compared between the two groups using a paired t test. The SPSS 13.0 statistical package was used for analysis with a significance level of $P < 0.05$. The error of RBF transformation was shown by shell-to-shell deviation between the final teeth and the scanned digital crowns (Fig. 5).

Generation of the dynamic masticatory system model

To build a dynamic masticatory model, mandible movement data recorded by the Arcus Digma system were used to drive

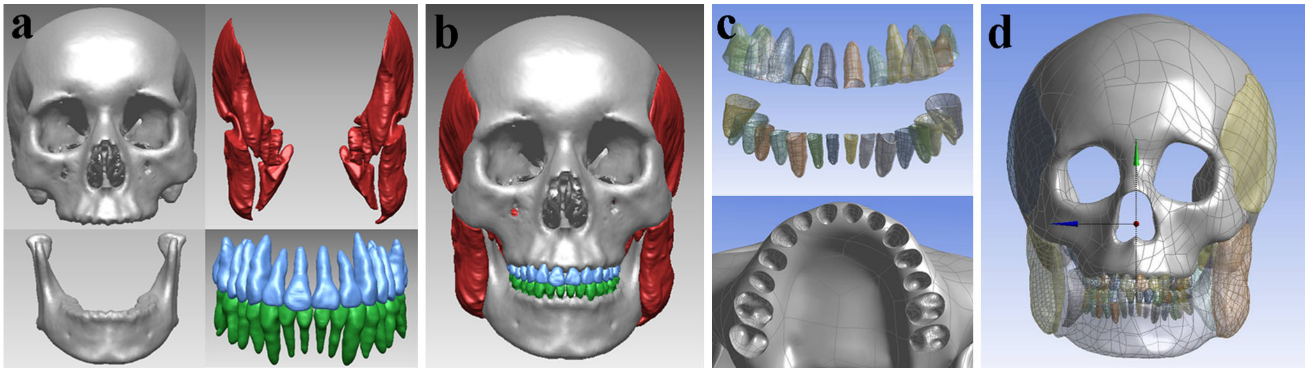

Fig. 3 **a** The segmented craniomaxilla, mandible, four pairs of masticatory muscles and 28 teeth. **b** The reconstructed 3D static masticatory model. **c** The generated 28 PDLs and alveolar fossa, **d** Geometries of final masticatory model for FE analysis

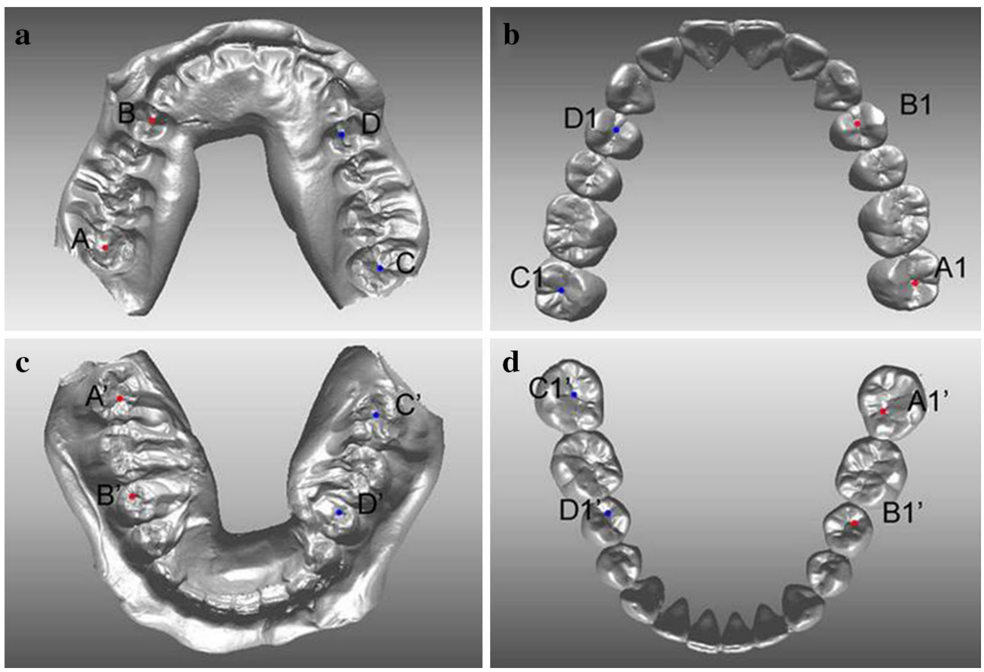

Fig. 4 *A*, *A*' are points on corresponding upper and lower teeth of DR group, and *A*', *A1*' are corresponding points of DC group; thus, *A–A*' and *A1–A1*' indicates corresponding inter-point distances in the DR and DC group; *B–B*' and *B1–B1*', *C–C*' and *C1–C1*', *D–D*' and *D1–D1*' are other examples of pairs of inter-point distances; the difference in inter-point distances between DR and DC group was calculated as the occlusion error

the static model. The keypoint was the registration of the global coordinates in two different systems. In the Rapidform software, the bite fork was registered onto the upper teeth using the upper cast–bite fork shell as the transfer medium. A local coordinate system was established, with the center point of the circular fork handle as the origin point, the long axis of the fork body as the X-axis, the short axis as the Z-axis, and the Y-axis perpendicular to the previous two axes. Then, the local coordinate system was translated superiorly by distance a and posteriorly by distance b ($a = 40$ mm and $b = 142$ mm, as recorded by the Arcus Digma system). Thus, the local coordinate system was transformed into the global coordinate system by alignment to match the coordinates of the Arcus Digma system (Fig. 6).

The TXT formatted data of the individual mandibular movements were imported into the mathematical software MATLAB 7.0 (Math Works Inc., MA., USA). The mandible was assumed to be rigid, and the translation and rotation of the mandible at any relative timepoint were calculated relative to the starting time. In the Transform Animate functional module of the Amira software, the levels of translation and rotation were input at sequential timepoints to conduct an animated simulation of mandibular movement.

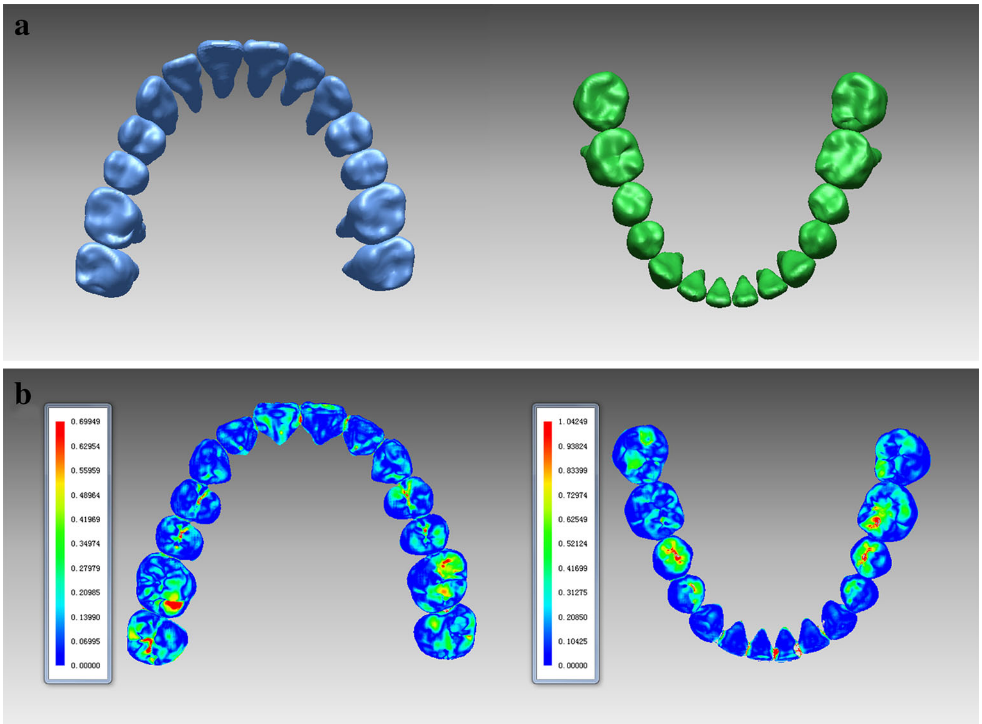

Fig. 5 **a** The final teeth after RBF transformation. **b** Shell-to-shell deviation between the final teeth crowns and the scanned digital crowns, and the mean deviation was 0.1 mm for both upper and lower arches

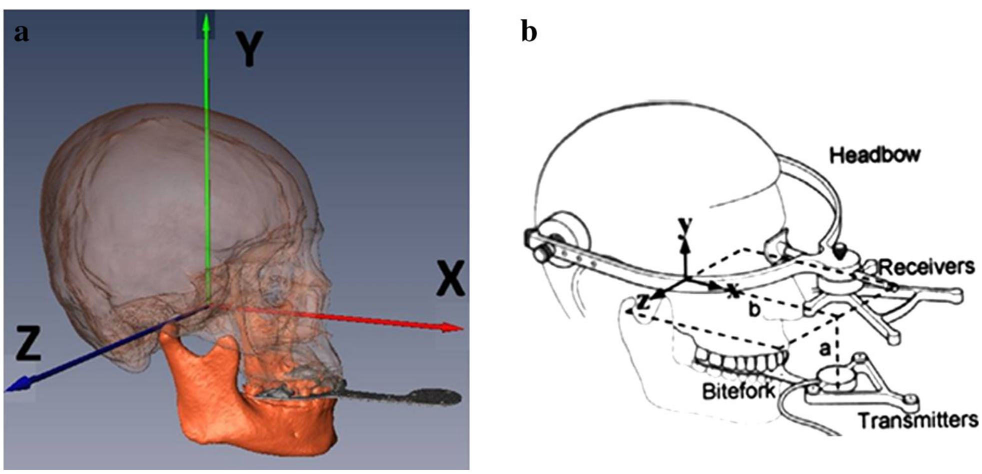

Fig. 6 Registration of the global coordinate system between the masticatory model (**a**) and the Arcus Digma system (**b**)

Generation of the FE masticatory system model

The components of the static masticatory system were imported into Geomagic Studio 12 (Raindrop Geomagic Inc., NC, USA). Periodontal ligament (PDL) was modeled as a uniform layer of 0.3 mm around the dental roots, and the alveolar fossa was formed by subtracting the volume of teeth and PDLs from the craniomaxilla and mandible (Fig. 3c). After triangle reduction, noise reduction, relaxation and grid-doctor processing, precise surfacing was performed, and the polygons were converted to NURBS (Non-Uniform Rational B-Splines) surfaces and exported as IGS files.

Then, the IGS files were imported into the FE modeling and analysis software Ansys 15.0 (ANSYS Inc., PA, USA). Sixty-six volumes, including the craniomaxilla, the mandible, 8 muscles, 28 PDLs and 28 teeth, were generated automatically (Fig. 3d). To be converted to the FE model, the volumes were meshed using Solid187 (10 tetrahedron nodes) as the element, and the quality of the mesh was verified.

Table 1 Mechanical properties of different components in the model

Material	Young's modulus (E) MPa	Poisson's ratio(γ)
Bone (craniomaxilla, mandible)	13,700	0.3
Teeth	20,000	0.3
PDL	12	0.45
	Constant c1 MPa	Constant c2 MPa
Muscle	0.01	0.01

Table 2 Muscle PCS, scaling factors, and vector coordinates utilized to model load sets for intercuspal clenching

Muscle	PCS (cm^2)	Scaling factors	Force (N)	Vector coordinates (N)-R		
				X	Y	Z
Superficial masseter	5.2	1.0	270.1	42.3	265.4	26.9
Deep masseter	2.1	1.0				
Medial pterygoid	4.0	0.76	148.0	19.1	129.4	−69.3
Anterior temporalis	4.4	0.98				
Middle temporalis	2.6	0.96	324.9	−179.8	255.4	89.2
Posterior temporalis	2.1	0.94				
Inferior lateral pterygoid	1.6	0.27	35.6	27.3	−2.3	−22.7
Superior lateral pterygoid	0.9	0.59				

$P = 0.37 \times 10^6 Nm^{-2}$; Force = PCS*P*Scaling factor; R right side; the left side of vector coordinates had the same X, Y but opposite Z value as the right side

The basic FE model included the craniomaxilla, mandible, 28 PDLs, and 28 teeth and consisted of 108737 tetrahedral elements and 160,163 nodes. The FE model was validated by comparing the bite force distribution of the whole teeth under masticatory muscle loading with that measured by T-Scan III (Tekscan Inc., USA). The mechanical properties of the components of the FE model were assumed to be linearly elastic, homogeneous and isotropic as a first approximation [11,15] (Table 1). The masticatory muscle loading conditions are described in Table 2, and the magnitude of each muscle force was assigned according to its total physiological cross section (PCS) and the scaling factors [16,17]. The origin and direction of each muscle force were defined from the attachment site and the long axis of the segmented muscle. Loading conditions were the same on both sides. The top surfaces of the craniomaxilla were fixed, and the translation of the mandible was constrained.

Masticatory muscle performances during mandibular opening

When simulating the masticatory muscle performance during mandibular movement, the FE model was simplified to the muscles and mandible. It consisted of 19,364 elements and 35,171 nodes. The mandible used the same mechanical property as above, and the muscles were assumed to be hyperelastic and isotropic (a Mooney–Rivlin material) (Table 1) [10]. The attachment surfaces of the muscles to the craniomaxilla were fixed. Mandibular displacement according to the individual mandibular movement data was used as the loading condition. Deformations and displacements of the masticatory muscles were simulated. Muscle forces generated at the timepoints of mouth opening of 2.3, 3.5, 5.0 and 6.3 mm were recorded.

Bite force analysis with orthodontic bite plate

In this part, we used the same FE model as the above basic masticatory system model, but the PDLs were mostly deleted leaving only 8 PDLs of teeth from the lower right first premolar to the lower left first premolar, and the position of mandible was adjusted according to the opening movement data at the four timepoints of mouth opening of 2.3, 3.5, 5.0 and 6.3 mm. A flat bite plate in the shape of a box and oriented vertical to the Y-axis was inserted between the upper and lower anterior teeth, and the contact between the bite plate and teeth was defined as the bonding contact. The thickness of the bite plate was set at 2.3, 3.5, 5.0 and 6.3 mm corresponding to the mouth opening degree, and the masticatory muscle force loading used the corresponding values calculated during simulating performances of masticatory muscles. The mechanical properties of the bite plate were defined to be the same as for bone, and the top surfaces of the bite plate were fixed. The bite force generated on the lower four incisors were analyzed. At the timepoint of mouth opening of 3.5 mm, the direction of bite plate was oriented vertical to the average

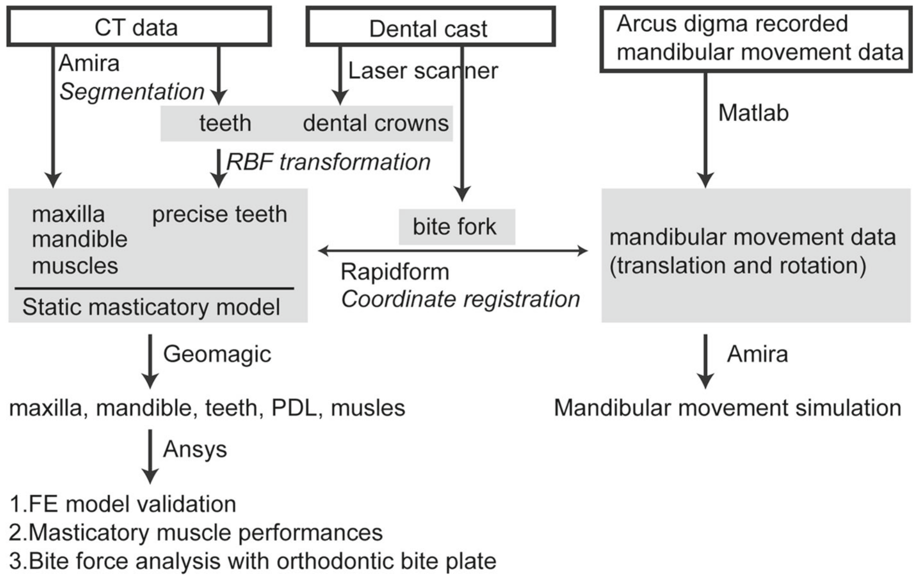

Fig. 7 Flowchart of the study

Table 3 A comparison of the inter-point distances (mm) between the DC and DR groups

Number	Inter-point distance		Difference	Mean	P
	DC group	DR group			
1	5.74	6.18	0.44	0.32 ± 0.25	0.003**
2	4.49	4.88	0.39		
3	4.58	4.34	−0.24		
4	5.38	5.51	0.13		
5	5.09	5.35	0.26		
6	4.39	4.76	0.37		
7	5.30	5.66	0.36		
8	4.63	5.36	0.73		
9	4.19	4.43	0.24		
10	2.53	3.02	0.49		

DC digital dental cast, *DR* digital occlusal relationship record.
** $P < 0.01$

long axis of the lower incisors; under the same muscle force loading, the bite force of the lower incisors were analyzed and compared.

A flowchart that shows the study design is presented in Fig. 7.

Results

Validation of the static masticatory system model

The error of occlusion can be observed in Table 3. The inter-point distances of the DR group were significantly greater than those of the DC group ($P < 0.01$). However, the relatively small mean difference (0.32 ± 0.25 mm) indicated that the static masticatory system model had good accuracy in occlusion. Teeth from the CT were transformed toward the scanned digital dental crowns using the RBF method; the mean shell-to-shell deviations between the final teeth crowns and the scanned digital crowns were 0.1 mm for both the upper and lower arches.

Simulation of individual mandibular movements

A 3D geometric model of an individual masticatory system was built, including the craniomaxilla, mandible, 4 pairs of masticatory muscles (bilateral temporalis, masseter, medial pterygoid and lateral pterygoid) and 28 complete teeth (from the central incisor to the second molar in four quadrants). Animated simulations of maximal interincisal opening, protrusion and lateral excursion were performed with the model and could be viewed from any perspective (Fig. 8).

Validation of the basic FE model

Using the bite force data of T-Scan III in the maximum intercuspal position as a reference, the bite force distribution solved out with the FE model was compared. Although there were differences with respect to specific teeth, especially the right first molar and second molar, the results of the FE model showed overall similarity to that of the T-Scan. The bite force was evenly distributed on the left and right sides (with the right side slightly heavier), and the bite force was mainly focused on the posterior molars (with the anterior teeth close to zero) (Fig. 9).

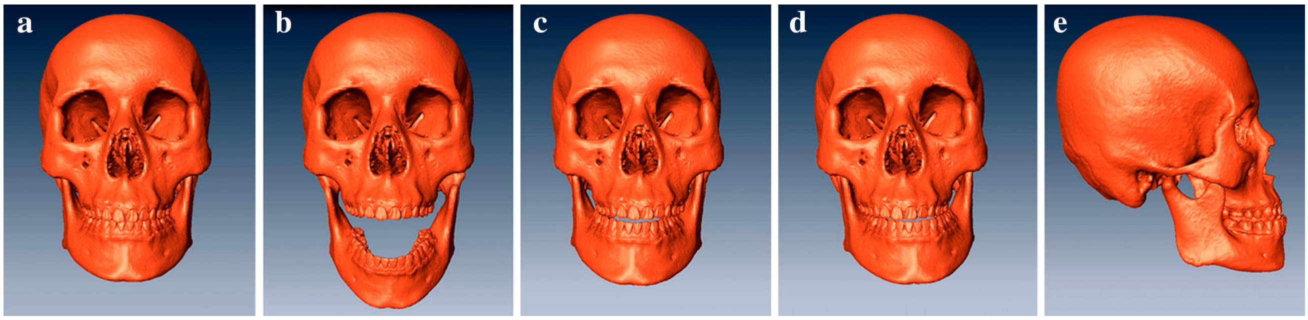

Fig. 8 Simulations of mandibular opening, lateral excursion and protrusion. **a** Static model in the maximum intercuspal position. **b** Opening movement. **c** Right excursion movement. **d** Left excursion movement. **e** Protrusive movement

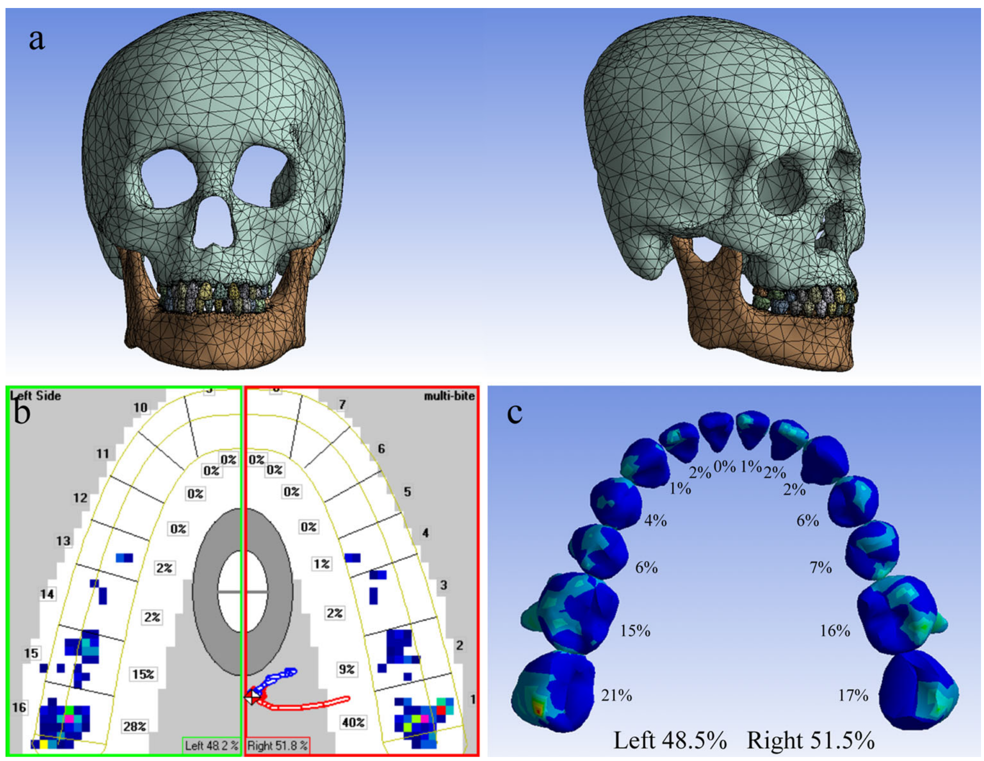

Fig. 9 **a** Mesh of the basic FE masticatory system model. **b** Bite force distribution measured with T-Scan. **c** Bite force distribution calculated with FE model

Masticatory muscle performance during mandibular opening

Under the loading of mandibular movement data, the masticatory muscles showed deformation and displacement during the open–close movements of the mandible. The displacement values of the mandible and muscles in Y-axis are depicted with a color distance map (Fig. 10b). Muscle force was recorded as the reaction force on the constrained muscle attachment surfaces (Fig. 10c). The muscle force values at the mouth opening of 2.3, 3.5, 5.0 and 6.3 mm are listed in Table 4. Muscle force increased with the increase in mouth opening; it concentrated on the direction of Y-axis; the highest value was generated by masseter; minor difference existed between the left and right sides.

Bite force analysis with orthodontic bite plate

Under the loading of the individual masticatory muscle force due to mouth opening, the bite forces generated on the lower four incisors when they rested on the bite plate (Fig. 11) are listed in Table 5. The direction of the resultant force was in accordance with the long axis of the tooth irrespective of the amount of mouth opening and the orientation of the bite plate. The resultant bite force was heavier on the lateral incisors than on the central incisors, and it increased with

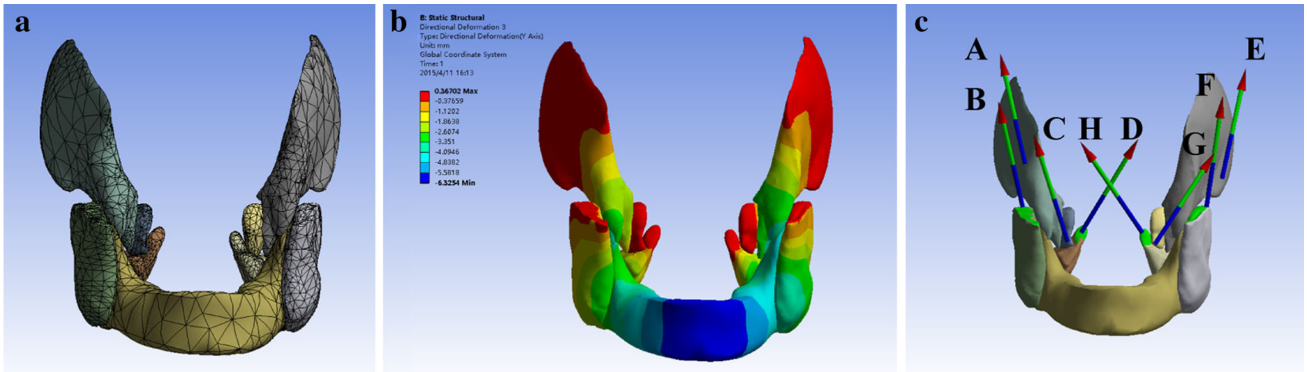

Fig. 10 **a** Mesh of the FE model for simulating muscle performance. **b** *Color distance map* showing the displacement of muscles and mandible on the *Y*-axis during opening movement (*red, min; blue, max*). **c** *Arrows* showing the muscle forces generated during opening movement (*A*, *E*: forces of temporalis; *B*, *F*: forces of masseter; *C*, *G*: forces of lateral pterygoid; *D*, *H*: forces of medial pterygoid)

Table 4 Muscle force generated with different amount of mouth opening

Mouth opening (mm)	Muscles	*X* (*N*)-R	*Y* (*N*)-R	*Z* (*N*)-R	*X* (*N*)-L	*Y* (*N*)-L	*Z* (*N*)-L
2.3	Masseter	0.74	2.07	0.64	0.36	2.70	−0.44
	Temporalis	−0.06	0.37	0.09	−0.10	0.66	−0.15
	Medial pterygoid	0.08	0.27	−0.17	0.12	0.42	0.34
	Lateral pterygoid	0.02	0.10	0.03	−0.03	0.07	−0.04
3.5	Masseter	1.21	3.28	0.91	0.68	4.12	−0.65
	Temporalis	−0.09	0.59	0.14	−0.14	1.02	−0.23
	Medial pterygoid	0.15	0.46	−0.29	0.22	0.65	0.49
	Lateral pterygoid	0.04	0.15	0.04	−0.03	0.10	−0.06
5.0	Masseter	1.69	4.81	1.18	1.03	5.70	−0.89
	Temporalis	−0.12	0.86	0.20	−0.19	1.44	−0.32
	Medial pterygoid	0.23	0.71	−0.44	0.33	0.94	0.67
	Lateral pterygoid	0.05	0.22	0.06	−0.04	0.15	−0.09
6.3	Masseter	2.07	6.12	1.42	1.27	7.15	−1.04
	Temporalis	−0.16	1.11	0.25	−0.24	1.84	−0.40
	Medial pterygoid	0.31	0.93	−0.57	0.42	1.21	0.83
	Lateral pterygoid	0.05	0.28	0.09	−0.06	0.19	−0.13

R right side, *L* left side

the increase of mouth opening (Fig. 12), but the values were nearly the same when the bite plate was oriented vertical to the *Y*-axis and vertical to long axis of the teeth.

Discussion

The human masticatory system is very delicate. Because it is the primary musculoskeletal component of the craniofacial area, its anatomical structure and function have been widely studied. However, due to the system's complexity, relatively few studies addressing its dynamics have been performed, despite the well-developed field of research describing the dynamics of other musculoskeletal systems such as the shoulder or leg.

The masticatory system has a complex architecture and includes many muscles of different shapes and sizes. Furthermore, the upper and lower jaws articulate through temporomandibular joints that have a complicated shape, and the teeth have various morphologies and positions. Apart from the intrinsic complexity of the system, there are limitations to the collection of masticatory function data. For example, some of the masticatory muscles run deep and are partially hidden behind bony structures, preventing easy access for electromyographic measurements.

The development of biomechanical models has provided an experimental framework to explore musculoskeletal sys-

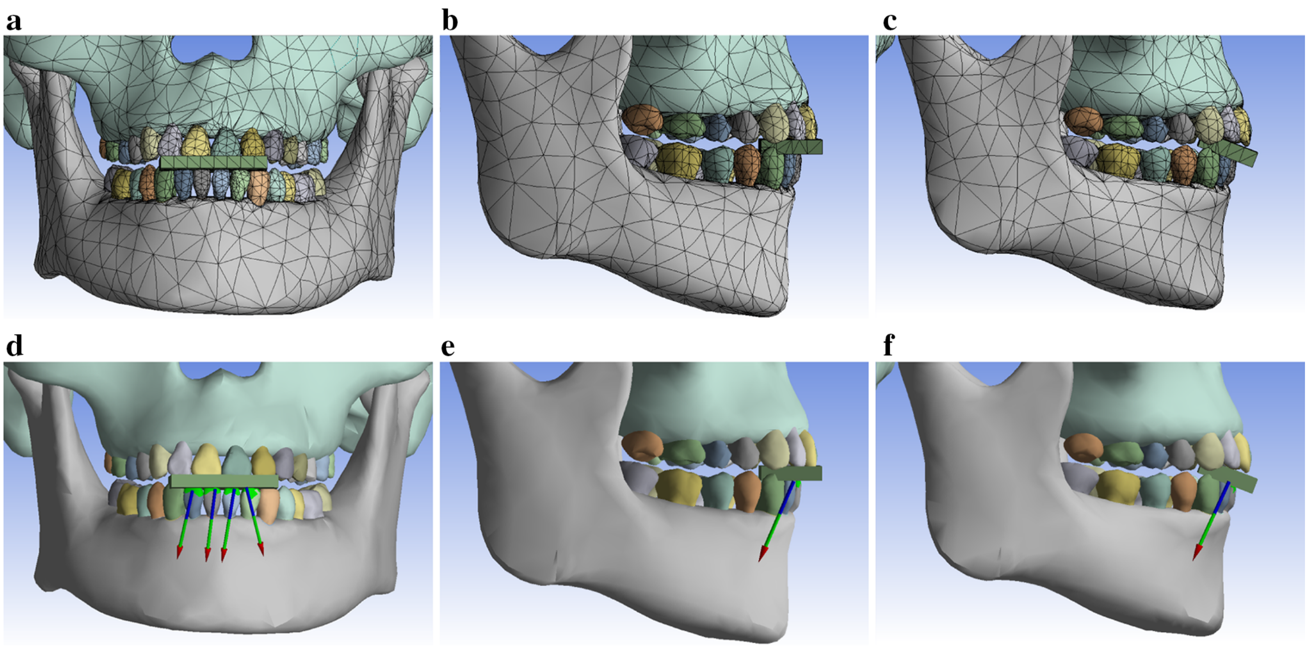

Fig. 11 **a**–**c** Mesh of the FE model for bite force analysis with the bite plate (**a**, **b** the bite plate was vertical to the Y-axis, **c** the bite plate was vertical to the long axis of the teeth). **d**–**f** Bite force generated on the lower incisors

Table 5 Bite force generated on the lower four incisors with different thicknesses and orientations of the bite plate

Thickness of the bite plate (mm)	Teeth	X (N)	Y (N)	Z (N)	Resultant (N)
2.3	31	−0.04	−0.12	0.01	0.13
	32	−0.17	−0.32	−0.10	0.38
	41	−0.06	−0.15	0.01	0.17
	42	−0.12	−0.22	0.03	0.25
3.5	31	−0.07	−0.20	0.03	0.21
	32	−0.27	−0.52	−0.15	0.60
	41	−0.11	−0.25	0.02	0.27
	42	−0.21	−0.37	0.07	0.43
5.0	31	−0.18	−0.34	−0.04	0.39
	32	−0.39	−0.65	−0.20	0.78
	41	−0.17	−0.37	0.03	0.41
	42	−0.36	−0.55	0.12	0.67
6.3	31	−0.23	−0.43	−0.07	0.49
	32	−0.53	−0.82	−0.30	1.02
	41	−0.23	−0.45	0.03	0.51
	42	−0.46	−0.64	0.16	0.80
3.5 (Vertical to long axis of tooth)	31	−0.08	−0.22	0.02	0.24
	32	−0.34	−0.55	−0.22	0.68
	41	−0.12	−0.25	0.06	0.29
	42	−0.27	−0.40	0.11	0.49

31, the lower left central incisor; 32, the lower left lateral incisor; 41, the lower right central incisor; 32, the lower right lateral incisor

tem dynamics without the drawbacks that accompany human testing. In this study, biomechanical modeling of the masticatory system was explored. Structural information from different sources was integrated through the comprehensive application of advanced 3D data processing software, ensuring the accuracy of the geometric masticatory system model. Using the occlusal relationship record as a standard, the difference between the inter-point distances of the DR and DC groups was calculated. That value, the mean modeling error of teeth occlusion, was only 0.32 mm. When considering the

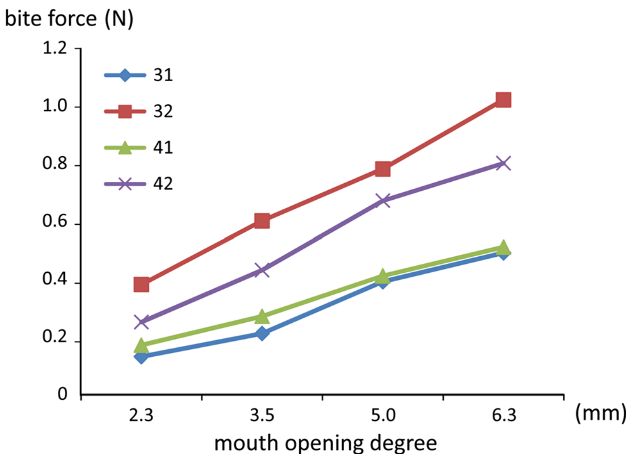

Fig. 12 Bite force generated on the lower four incisors during different amounts of mouth opening. 31, the lower left central incisor; 32, the lower left lateral incisor; 41, the lower right central incisor; 42, the lower right lateral incisor

point identification error and the thickness of the polysiloxane material used to cast the occlusal relationship record, the actual occlusion error is likely even lower. Furthermore, the deviation between the final teeth acquired using the RBF transformation method and the scanned high-accuracy dental crowns was only 0.1 mm. With these two sources of error added, the static masticatory model had an accuracy of no more than 0.5 mm in occlusion.

Dynamic simulations of mandibular movement require a combination of a 3D digital masticatory model and individual mandibular movement data [18]. In the past, mandibular movement has been studied using only two-dimensional trajectories of incisal or condylar points, but now it can be recorded with various jaw movement analyzers [12,13]. This study used the 3D Arcus Digma system [19], which has high accuracy to 0.1 mm and 1.5 °. Assuming that the mandible is a rigid body without deformation during movement [17], the sequential coordinates of the three landmarks were converted into values for the translation and rotation of the mandible within the global coordinate system. The different coordinate systems that had to be registered before the mandibular movement data could be applied to the mastication model. The bite fork, which was scanned and bound to the upper jaw to ensure accuracy, was used as the key medium for registration. Finally, the animated simulation of individualized mandibular movements was achieved and could be observed from any perspective. This simulation might improve our understanding of the physical functions of the mandible and the joint and might facilitate doctor–patient communication if any abnormalities in mandibular movement exist.

The 3D FE method is a powerful tool for solving biomechanical problems. In recent years, it has been introduced to study stress/strain in the temporomandibular joint [11] and mandible [15] during loading caused by muscle force. Because of the difficulties in precise muscle reconstruction, for static FE model analysis, the magnitude of the muscle force is usually estimated according to the physiological cross-sectional area and adjusted by the intensity of myoelectric activity [16,17]. When validating the basic masticatory system model, we used a similar muscle force loading methodology. In this study, CT image-based reconstruction of the masticatory muscles was used. The maximum cross-sectional area was acquired from CT scan. The muscle outlines could be clearly distinguished in the CT images, particularly at the anatomical borders between the jaw and the muscles, where the muscles attach. Thus according to the attachment areas and major axis of the segmented muscles, the loading sites and direction of muscle force could be individually achieved. Using the bite force data from T-Scan as a reference, the bite force distribution among the teeth rather than the absolute force value was considered. The bite force distribution calculated from the FE model displayed a similar result to that from T-Scan and indicated that the static FE model was acceptable. The bite force percentage was obviously higher for the right second molar in the T-Scan result, and abnormally high occlusal points might have existed locally. Moreover, the wedging effect when biting on the testing membrane of T-Scan may explain the bite force of zero for the anterior teeth to some extent.

The functional activities of the masticatory muscles are closely related to mandibular movements and the bite force [20]. In simulating performances of masticatory muscles along with mandibular movement, a hyperelastic and isotropic behavior was used for masticatory muscles and the muscles were assumed to be passively stretched. Rohrle [10] developed a 3D geometric model of both the jaw and the masticatory muscles based on the Visible Man project and converted it into an FE model. The masseters were modeled to be hyperelastic and transversely isotropic material. Using mandibular movement data from a volunteer, he simulated the deformation of the masseters and solved for the muscle force during mastication. Compared with his study, our method emphasized the establishment of an individual functional masticatory model based on a living subject. The anatomical structure and mandibular movement data were obtained from the same individual, which improved the accuracy and consistency of both the static and dynamic models. The performances of the masticatory muscles during mandibular open–close movements were simulated. Although the masticatory muscles are contracting and deforming themselves and are not being altered by the movement of the mandible, coordinating their performance with mandibular movements will further elucidate their individual biomechanical behaviors.

The masticatory muscle force acquired in simulating its performance along with the mandibular opening was used as a corresponding loading to analyze the bite force on the lower incisors with different thicknesses and different orientations of the orthodontic bite plate. The results indicated that the bite force was in accordance with the long axis of the tooth, irrespective of the bite plate thickness and orientation. The bite force value increased with increased bite plate thickness; however, it was not influenced by the bite plate orientation. Clinical observations revealed that the lower incisors could be intruded with a force of 20 g per tooth [21], and this value was between the bite force values on the central incisors with the bite plate of 2.3 and 3.5 mm. The findings may facilitate designing orthodontic bite plate, and a thickness of approximately 3 mm may be appropriate for both intruding the incisors and alleviating patient discomfort with a relatively thinner bite plate.

For a more accurate FE analysis, the established masticatory model must be further improved by adding the articular disk of the temporomandibular joint, the non-uniform periodontal membrane and the fiber distributions within muscles capable of active and passive muscle behavior. These data can be obtained from individual high-resolution MRI scans. Additionally, the individual material properties of the different components of the model should be considered.

Conclusions

In this study, a 3D masticatory system model composed of the craniomaxilla, the mandible, 4 pairs of primary masticatory muscles, 28 PDLs and 28 complete teeth was developed by integrating 3D images from different sources using advanced 3D data processing software. Individualized mandibular movements corresponding to opening, protrusion and lateral excursion were simulated in this model. Deformation and displacement of the masticatory muscles along with the individual mandibular movements were modeled with the FE method. The bite force generated on the lower incisors with different thicknesses and orientations of the orthodontic bite plate were analyzed, and the results suggested that a thickness of 3 mm may be appropriate for clinical use.

Acknowledgments We thank Dr. Qiufei Xie (Professor in the Department of Prosthodontics, Peking University School and Hospital of Stomatology) for recording the volunteer's mandibular movement data with the Arcus Digma system. We are also grateful to Wenlong Li (Postgraduates of Spacecraft Design, Beihang University School of Astronautics) for technological support with the MATLAB software. This study was supported by the National Natural Science Foundation of China under Grants No.81200806 and No.81241036.

Compliance with ethical standards

Conflict of interest Fanfan Dai, Longfang Wang, Gui Chen, Si Chen and Tianmin Xu declare that they have no conflict of interest.

Ethical statement This study was reviewed and approved by the Ethics Committee of Peking University School and Hospital of Stomatology. All procedures followed were in accordance with the ethical standards of the responsible committee on human experimentation (institutional and national) and with the Helsinki Declaration of 1975, as revised in 2008 (5). The written informed consent was obtained from the subject included in this study.

References

1. Southard TE, Behrents RG, Tolley EA (1990) The anterior component of occlusal force, part 2: relationship with dental malalignment. Am J Orthod Dentofacial Orthop 97(1):41–44
2. Acar A, Alcan T, Erverdi N (2002) Evaluation of the relationship between the anterior component of occlusal force and postretention crowding. Am J Orthod Dentofacial Orthop 122(4):366–370
3. Forsberg CM, Hellsing E (1984) The effect of a lingual arch appliance with anterior bite plane in deep overbite correction. Eur J Orthod 6(2):107–115
4. Ingervall B, Helkimo E (1978) Masticatory muscle force and facial morphology in man. Arch Oral Biol 23:203–206
5. Van Spronsen PH, Weijs WA, Valk J, Prahl-Andersen B, Van Ginkel FC (1989) Comparison of jaw-muscle bite-force cross-sections obtained by means of magnetic resonance imaging and high-resolution CT scanning. J Dent Res 68(12):1765–1770
6. Helkimo E, Carlsson GE, Helkimo M (1977) Bite force and state of dentition. Acta Odontol 35(6):297–303
7. Helkimo EVA, Carlsson GE, Carmeli Y (1975) Bite force in patients with functional disturbances of the masticatory system. J Oral Rehabil 2(4):397–406
8. Throckmorton GS, Rasmussen J, Caloss R (2009) Calibration of T-Scan® sensors for recording bite forces in denture patients. J Oral Rehabil 36(9):636–643
9. Suzuki T, Kumagai H, Watanabe T, Uchida T, Nagao M (1997) Evaluation of complete denture occlusal contacts using pressure-sensitive sheets. Int J Prosthodont 10(4):386–391
10. Röhrle O, Pullan AJ (2007) Three-dimensional finite element modeling of muscle forces during mastication. J Biomech 40(15):3363–3372
11. Savoldelli C, Bouchard PO, Loudad R, Baque P, Tillier Y (2012) Stress distribution in the temporo-mandibular joint discs during jaw closing: a high-resolution three-dimensional finite-element model analysis. Surg Radiol Anat 34(5):405–413
12. Otake Y, Suzuki N, Hattori A, Shigeta Y, Ogawa T, Fukushima S, Uchiyama A (2006) Real-Time Mandibular movement analysis system using four-dimensional cranial bone model. Syst Comput Jpn 37(8):1–11
13. TerajimaM Endo M, Aoki Y, Hayasaki H, Goto TK, Nakasima A (2008) Four-dimensional analysis of stomatognathic function. Am J Orthod Dentofacial Orthop 134(2):276–287
14. Seol Y, Seo J, Kim PH, Lewis JP, Noh J (2011) Artist friendly facial animation retargeting. ACM Trans Graph 30(6):162
15. Ichim I, Kieser JA, Swain MV (2007) Functional significance of strain distribution in the human mandible under masticatory load: numerical predictions. Arch Oral Biol 52(5):465–473
16. Koolstra JH, Van Eijden T, Weijs WA, Naeije M (1988) A three-dimensional mathematical model of the human masticatory system predicting maximum possible bite forces. J Biomech 21(7):563–576
17. Korioth TWP, Hannam AG (1994) Deformation of the human mandible during simulated tooth clenching. J Dent Res 73(1):56–66
18. Bisler A, Bockholt U, Kordass B, Suchan M, Voss G (2002) The virtual articulator. Int J Comput Dent 5(2–3):101–106
19. Pröschel P, Morneburg T, Hugger A, Kordass B, Ottl P, Niedermeier W, Wichmann M (2002) Articulator-related registration-a simple concept for minimizing eccentric occlusal errors in the articulator. Int J Prosthodont 15(3):289–294

20. Yang Y, Foong KWC, Ong SH, Yagi M, Takada K (2012) Image-based estimation of biomechanical relationship between masticatory muscle activities and mandibular movement. In: IEEE 12th international conference on bioinformatics & bioengineering (BIBE)
21. Bench RW, Gugino CF, Hilgers JJ (1977) Bioprogressive therapy, part 2: principles. J Clin Orthod 12(2):661–682